

Efficient SMN rescue following subcutaneous tricyclo-DNA antisense oligonucleotide treatment

Valérie ROBIN^{(1)*}, Graziella GRIFFITH⁽¹⁾, John-Paul L. Carter⁽¹⁾, Christian J. LEUMANN⁽²⁾, Luis GARCIA⁽¹⁾, Aurélie GOYENVALLE^{(1)*}

(1) Université Versailles Saint Quentin, INSERM U1179, 78180 Montigny-le-Bretonneux, France.

(2) Department of Chemistry & Biochemistry, University of Bern, CH 3012 Bern, Switzerland.

*corresponding author:

Valérie ROBIN and Aurélie GOYENVALLE

U1179 équipe Biothérapies des maladies neuromusculaires

UFR des sciences de la santé

Avenue de la source de la bièvre

78180 MONTIGNY LE BRETONNEUX

France

+33 1 70 42 94 30

valerie.robin@uvsq.fr

aurelie.goyenvalle@uvsq.fr

ABSTRACT

Spinal muscular atrophy (SMA) is a recessive disease caused by mutations in the *SMN1* gene, which encodes the protein Survival Motor Neuron (SMN) whose absence dramatically affects the survival of motor neurons. In humans, the severity of the disease is lessened by the presence of a gene copy, *SMN2*. *SMN2* differs from *SMN1* by a C-to-T transition in exon 7, which modifies pre-mRNA splicing and prevents successful SMN synthesis. Splice-switching approaches using antisense oligonucleotides (AON) have already been shown to correct this *SMN2* gene transition providing a therapeutic avenue for SMA. However, AON administration to the central nervous system (CNS) presents additional hurdles. In this study we show that systemic delivery of tricyclo-DNA (tcDNA) AON in a type III SMA mouse augments retention of exon 7 in *SMN2* mRNA both in peripheral organs and the CNS. Mild type III SMA mice were selected as opposed to the severe type I model in order to test tcDNA efficacy and their ability to enter the CNS after maturation of the BBB. Furthermore, subcutaneous treatment significantly improved the necrosis phenotype and respiratory function. In summary, our data support that tcDNA oligomers effectively cross the blood-brain-barrier and offer a promising systemic alternative for treating SMA.

Key words

Splice switching, Spinal muscular atrophy, antisense oligonucleotide, tricyclo-DNA

INTRODUCTION

Spinal muscular atrophy (SMA) is an autosomal-recessive inherited disease characterised by the degeneration of α -motor neurons of the anterior horn of spinal cord which leads to progressive muscle atrophy. It is caused by mutations in the gene *SMN1* encoding the Survival Motor Neuron protein (SMN) and it has an incidence of about 1 in 6,000 live births.¹ SMN is a 37 kDa protein located in both the cytoplasm and the nucleus where it is concentrated in several intense foci referred to as Gemini or Cajal Bodies (gems).² This ubiquitous protein plays an essential role in uridine-rich small nuclear ribonucleoprotein (snRNP) assembly in the cytoplasm,³ and also participates in snRNP importation into the nucleus. Once in the nucleus SMN relocates to gems, while released snRNPs accumulate in Cajal bodies to form part of the splicing machinery. One might expect that reduced SMN levels should broadly affect the processing of pre-mRNAs in all cell types, though this clearly does not occur in SMA patients. The neuron-specific consequences of SMA are still widely debated, though have been partially attributed to SMN's role in the axonal transport of particular mRNAs which suggests a rationale for the prominent effect of SMN-depletion on spinal motor neuron survival.⁴ The clinical consequences of SMA range from severe to mild (types 1-4), tending to affect proximal muscle groups primarily, and with deleterious effects on respiratory function.

In humans, the severity of disease is lessened by the presence of *SMN2* (a centromeric copy of the gene).⁵ *SMN2* differs from *SMN1* (a telomeric copy) by only one nucleotide in the coding sequence: a translationally-silent C to T at position +6 (C6T) altering the splicing of exon 7. Consequently 10% of *SMN2* pre-mRNAs are correctly spliced but 90% lack exon 7 (SMN(Δ 7)).^{6,7} Translation of respective mRNAs gives rise to a very limited amount of fully-

functional full-length SMN protein in addition to a truncated SMN Δ 7) protein which is rapidly degraded.^{8,9} As one might expect, the severity of SMA is inversely-proportional to the *SMN2* copy number which varies from 1 to 8 in humans;¹⁰ suggesting the potential of SMN2 correction as a valid therapeutic strategy.

The splicing of *SMN2* exon 7 has been well characterised and requires many different elements including: a suboptimal intron 6 branch point;¹¹ an extended inhibitory context;^{12,13} a conserved tract domain, an inhibitory 3'-cluster;¹² an intronic silencer element in intron 7 (ISS-N1)¹⁴ and a terminal stem-loop structure on 5' splice site exon 7 (TSL)¹⁵ (**Supplementary fig. S1**). The particular genomic organisation of *SMN* genes has enabled novel therapeutic approaches aiming at re-including SMN2 exon 7 to produce fully-functional SMN protein in the absence of the *SMN1* gene. This has already been achieved using antisense-oligonucleotide (AON) strategies aimed at: blocking the exonic splice-silencer generated by the C6T transition; annealing the intronic splice silencer downstream of exon 7; or decreasing the strength of the acceptor splice site of exon 8.¹⁶

Various classes of AON have been developed to modulate mRNA splicing. Oligonucleotide studies have shown efficient re-inclusion of *SMN2* exon 7, in particular those using 2'-OMethoxyEthyl (2'MOE) with 17 mer AONs targeting ISS-N1. This particular AON demonstrated phenotypic rescue (ear and tail necrosis) of type III SMA mice (a mild phenotype) after intracerebroventricular (ICV) injection,¹⁷ and increased survival of type I SMA mice (a severe model) by subcutaneous injections at P0 and P3.¹⁸ Studies have also been conducted using phosphorodiamidate morpholino oligomer (PMO) AONs on different mice models using ICV injection that result in a significantly extended life-span.^{19,20} Interestingly a cumulative benefit was obtained when ICV injections were coupled with intraperitoneal injections (IP) further reinforcing the peripheral function of SMN in SMA mice, previously demonstrated by Hua and colleagues.^{18,21} This peripheral role of SMN

strongly suggests that the optimal biodistribution of AONs across tissue types is important for therapeutic efficacy (at least in SMA mice models).

Notwithstanding these advances in chemistry and design, the uptake of AONs is still limited in many tissues including the heart and the CNS – a crucial target in SMA. This is due to the inability of most AONs to cross the blood-brain-barrier (BBB). Accordingly, in the majority of SMA animal studies and in trials for the recently U.S. Food and Drug Administration (FDA)-approved nusinersen (an AON targeting ISS-N1), treatment is administered via the intrathecal or ICV route. Despite encouraging data, these routes of administration present obvious clinical challenges and neglect the issue of delivery of AONs to the periphery.

In this paper we explore the therapeutic potential of tricyclo-DNA AONs (tcDNA), a class of conformationally-constrained DNA analogues that display enhanced binding properties to DNA and RNA,²² allowing them to be designed as shorter sequences compared with chemistries such as 2'MOE or PMO. Moreover tcDNA were recently shown to cross the BBB,²³ a key property which allows us to effectively evaluate the central and peripheral restoration of SMN following systemic delivery.

In our study we first compare the efficacy of two different tcDNA sequences to induce exon 7 re-inclusion *in vitro*. We further investigate the *in vivo*-efficacy of tcDNA in a mild SMA mouse model (type III SMA mouse) to induce exon re-inclusion in all tissues following systemic administration. We have selected the type III SMA mouse model in order to test tcDNA-AONs efficacy, and their ability to enter the CNS after maturation of the BBB.²⁴ This would not have been feasible with severe type I mice which require injections around P0-P2 because of their very short lifespan (around P10).^{17, 18}

After subcutaneous tcDNA treatment we show efficient exon re-inclusion in all tissues including the CNS, which leads to phenotypic improvement in type III SMA. Furthermore,

for the first time in SMA mice we describe rescue of respiratory function after treatment with tcDNA using whole-body plethysmography.

RESULTS

TcDNA AON effectively restores exon 7 reinclusion in SMA type-1 fibroblasts

To evaluate the efficacy of tcDNA AONs SMA type-1 fibroblast cells (GM03813, Coriell) were transfected with 30µg of oligonucleotide targeting the downstream ISS-N1 site in intron 7, thereby improving the strength of the 5' donor site (15 mer tcDNA-AON I7; henceforth referred to as 'TCI7'). Total RNA from transfected fibroblasts was analysed by reverse transcription PCR (RT-PCR) 48h after transfection to establish the inclusion levels of SMN2 exon 7. In TCI7-treated SMA fibroblasts the level of exon 7 inclusion was augmented to 64% from a baseline of 40% in untreated SMA fibroblasts (**fig. 1a**).

Despite the fact that SMA type-1 fibroblasts cells have no functional SMN1 gene and only two copies of SMN2 gene, they still produce SMN protein generated from the two existing SMN2 gene copies, however, the truncated protein of the SMN2 gene is unstable and rapidly degraded, hampering normal cellular function. Western blot was conducted and protein levels were recorded as a percentage of total actin expressed by respective fibroblast cell lines (GM03814, Coriell) (**fig. 1b, WT**). Untreated SMA type-1 fibroblasts expressed 10% of SMN protein at 37 kDa (**fig. 1b, SMAI**) whereas in TCI7-treated type-1 SMA fibroblasts induced a significant increase of total SMN protein reaching mean levels of 90% as a proportion of total WT levels (**fig. 1b, TCI7**).

In addition, another tcDNA oligonucleotide sequence (17 mer tcDNA-AON TSL; henceforth referred to as 'TCTSL') which anneals to the structure of terminal stem-loop (TSL;

supplementary fig. S1) was investigated, and analogous 2'O-Methyl compounds were looked at to compare their efficacies (**Supplementary fig. S2**). RT-PCR and western blot results indicate that tcDNA AONs induce higher levels of exon 7 inclusion and SMN protein restoration compared to 2'OMe AONs (although not statistically significant). Regarding the targeted region, ISS7-N1-manipulation with AONs resulted in more inclusion of exon 7 and SMN protein expression which prompted us to continue with this target for the remaining experiments.

To assess proper localisation of SMN protein in gems immunofluorescence was used. Compared with fibroblasts of healthy individuals normally displaying between 52-113 gems/100 nuclei,²⁵ most SMA type I patient fibroblasts have very limited amounts of SMN-containing nuclear gems (**figs. 1c and 1d**). To determine if TCI7 treatment increased levels of full-length SMN protein in its correct localisation we counted the number of gem-positive nuclei in treated and untreated SMA type-1 fibroblasts. As shown in figure 1c the restored SMN protein is correctly localised in nuclear gems in TCI7-treated fibroblasts and that the number of gem positive nuclei is restored to the level found in fibroblasts of healthy individuals (**fig. 1d**).

TCI7 induces exon 7 inclusion in SMA type III mice

Our *in vivo* studies were conducted using SMA type III transgenic mice which exhibit a mild SMA phenotype. Type III SMA mice are knocked out for murine *SMN* and possess 2 transgenes comprising 2 copies of the human *SMN2* gene leaving a total of 4 copies of *SMN2* genes (*Smn*^{-/-}; *SMN2* ^{+/+}).²⁴ Type III SMA mice were injected subcutaneously every week for a period of 4 or 12 weeks with a dose of 200mg/kg of TCI7 (or PBS as a control in the untreated mice) and sacrificed 2 weeks post-treatment. Since an element of our enquiry is to

establish trans- blood-brain-barrier (BBB) efficacy, the injection of mice commenced at P7 because at this stage of murine development the BBB already has very limited permeability.

Mice were analyzed for exon 7 inclusion by RT-PCR in different tissues including the gastrocnemius, diaphragm, heart, brain, and the spinal cord (**fig. 2**). In untreated mice the percentage of exon 7 inclusion in different tissues measured approximately 30%. TCI7 treatment significantly increased the inclusion of exon 7 in all tissues. This increase was particularly significant in the gastrocnemius muscle where 55% of exon 7 inclusion is detected after 4 weeks of treatment and 75% after 12 weeks of treatment. The degree of improvement was similar in diaphragm, heart and spinal cord with close to 50% inclusion after 4 weeks of treatment and up to 60% inclusion after 12 weeks. In brain the level of exon 7 inclusion reached about 40% after 12 weeks of treatment.

We also quantified by real-time quantitative RT-PCR (qRT-PCR) the level of inclusion in heart and brain tissue (**fig. 3**). In cardiac muscle qRT-PCR revealed that exon 7 inclusion was increased by 1.8-fold after 4 weeks of treatment and by over 2-fold after 12 weeks of treatment, confirming our previous semi-quantitative results. In the brain the inclusion was increased by 1.3 fold after 12 weeks of treatment verifying the ability of TCI7 to induce exon 7 inclusion in this tissue type.

TCI7 treatment is consistently sustained long-term

To evaluate the long term effect of tcDNA treatment we also analysed exon 7 inclusion by RT-PCR 10 weeks after the end of a 4 week course of tcDNA treatment, comparing it with samples obtained 2 weeks after the end of the treatment. The level of exon 7 inclusion appears to be similar for the two treated groups of mice at 2 weeks or 10 weeks after the end of the treatment across analysed tissues, suggesting that TCI7 or its effects persist in tissues for at least 10 weeks and are still inducing exon inclusion (**fig. 4**).

TCI7 treatment significantly improves respiratory function in SMA mice

SMA type III patients display respiratory dysfunction e.g. thoraco-abdominal asynchrony that is often caused by paralysis of the rib cage muscles in the presence of normal diaphragmatic activity.²⁶ Notwithstanding, to our knowledge respiratory function has never been studied in SMA type III mice. We investigated respiratory function in SMA type III mice by whole-body plethysmography, a non-invasive technique which measures various respiratory parameters (displayed in table 1). Compared with age-matched wild-type control FVB mice, Te (expiration time), RT (relaxion time) and Penh are significantly increased in SMA type III mice (**table 1**). Some parameters are not altered in SMA type III mice such as Ti (inspiration time), f (breathing frequency), TV (tidal volume) and MV (minute ventilation), consistent with what is observed in patients compared vs. healthy individuals²⁶ (**table 1**). TCI7 treatment in SMA type III mice restored RT and Te back to WT levels, suggesting that an increase of exon 7 inclusion to 60% in diaphragm is correlated with an improvement in respiratory function (**fig. 5**).

TCI7 treatment halts tissue necrosis in SMA III mice

Finally we investigated the effect of TCI7 treatment on the SMA III phenotype. SMA type III mice typically display progressive necrosis of tails, ears and toes.²⁴ Tail lengths in all mice were measured weekly throughout the course of treatment (12 weeks). Untreated mice at week 12 post-treatment underwent complete tail necrosis while treated SMA mice were unaffected (**fig. 6a,b,d**). Interestingly treatment with 200 mg/kg of TCI7 for 4 weeks also resulted in comparable tail lengths vs. mice treated for 12 weeks (**fig. 6d**), suggesting that this phenotypic benefit is sustained long-term. Moreover none of the treated mice presented necrosis of toes and ears at 12 weeks of age compared to SMA controls (**fig. 6b,c**). A dosing

regimen of 100 mg/kg was also evaluated resulting in slightly shorter tails vs the mice treated with 200mg/kg, suggesting that the effect of TCI7 is dose-dependent (data not shown).

DISCUSSION

Splice-switching to induce SMN-reinclusion using AON is a well-established strategy for the treatment of SMA. As previously mentioned, an AON of the 2'OMethoxyethyl-subtype named nusinersen (marketed as 'Spinraza') has recently been approved by the FDA for the treatment of SMA. After positive phase I results with an improvement of the Hammersmith Functional Motor Scale at 3 months post treatment,²⁷ interim analyses of phase 3 studies (ENDEAR and CHERISH) have demonstrated promising outcomes for patients. However, it is notable that nusinersen is administered intrathecally, a route of administration that is frequently less well-tolerated and typically requires specialist training vs. alternative routes of administration (e.g. subcutaneous or IV). In a study analysing the patient experience of nusinersen 32% of lumbar punctures (LP) resulted in adverse events.²⁸ Whilst the LP event rate in SMA patients is not shown to be higher than usually reported in children, it is noteworthy that all patients in this trial underwent general anaesthesia, which is not without its own risks.

CNS delivery of most AONs does not occur with systemic (e.g. intravenous or subcutaneous) injection. In SMA it is necessary for treatment to reach the CNS. To surmount the issue of AONs crossing the BBB ICV injections can be administered, or intrathecal pumps may be used clinically to deliver treatment to the spinal cord in patients. In the case of nusinersen intrathecal injection is crucial since it is unable to cross the BBB, though this neglects the issue of oligonucleotide penetration of peripheral tissues. It has been demonstrated several times (albeit in animal models) that peripheral rescue in SMA is important and that CNS

treatment alone is not sufficient. Whilst this phenomenon may not directly apply to human forms of the disease it remains an unaddressed issue.

Consequent to these challenges we believe that an unmet need remains for an AON treatment in SMA which not only deals with the issue of peripheral and central tissue penetration but also provides a simpler route of administration which is more easily administered and better tolerated. Previous research in our group using a Duchenne Muscular Dystrophy mouse model (named *mdx*) has demonstrated that tcDNA is able to cross the blood brain barrier.²³ Using tcDNA administered intravenously, *mdx* mice benefitted from an improvement in cardio-respiratory function and furthermore, correction of behavioural features controlled by central mechanisms. Given tcDNA's proven ability to cross the BBB whilst maintaining efficacy in the periphery when administered systemically, it is a strong candidate as a treatment for SMA.

To properly investigate this intrinsic property of tcDNA in SMA we elected to use type III SMA mice rather than the more severe type I mouse model to allow sufficient time for maturation of the BBB. After successful in-vitro proof-of-concept studies in SMA patient fibroblast cell lines, we have shown that subcutaneous administration of TC17 in type III SMA mice (at P7) induces significantly increased levels of exon 7 re-inclusion in all examined tissues. Importantly TC17 penetration includes the CNS demonstrating the ability of tcDNA to cross the blood brain barrier.

The TC17 splice-switching treatment improves the SMA phenotype by preventing tail, ear and toe necrosis, further implying therapeutic potential in SMA. It remains unclear why necrosis phenotypes are associated with SMA, a feature more prevalent in SMA mice than in human SMA phenotypes. The Hsieh-Li-model used here presents with necrosis of the tail, ears and toes, and many therapeutic studies conducted on severe forms of SMA mice report such events when lifespan is increased.^{19, 20, 29, 30} There are few documented cases of SMA

type I patients with a single copy of *SMN2* that have presented with finger necrosis, but the aetiology is unclear.^{31, 32} Parson's group has demonstrated that the dense capillary bed of skeletal muscle is dramatically decreased in severe SMA mice, potentially exacerbating the already-affected muscle. This mechanism of capillary reduction may also explain necrosis in mild SMA mice,³³ however the precise role of SMN protein in necrosis is not established, and may be due to a defect in innervations.³⁴ Some oligonucleotide studies delay this necrosis phenotype via ICV injection, and a recent study demonstrated a rescue of necrosis following subcutaneous injection between P23 and P31 after the onset of tail-tip necrosis.^{17, 35} These data demonstrate that the phenotype can be rescued by central administration, but also that restoration of the periphery is achievable via systemic administration.^{36, 37}

A further peripheral consequence of SMA is its respiratory complications, generally linked to intercostal muscle weakness and thoracic cage deformation.²⁶ In some patients atelectasis is reported,^{38, 39} and structural lung damage is observed after autopsy. In severe SMA mice lung abnormalities are also found.⁴⁰ For the first time, in this study we have investigated respiratory function in type III SMA mice, and also report some dysfunction. Interestingly, TCI7 treatment restores some parameters of respiration, which could reflect the increased level of exon 7 re-inclusion in diaphragm. Given TCI7's efficacy in the brain and spinal cord one cannot exclude the cause of this to restoring CNS control of respiration.

As previously demonstrated in the *mdx* model, we show here that tcDNA has excellent uptake in cardiac muscle, with similar levels of exon re-inclusion to that of diaphragmatic tissue. Whilst cardiac issues are not particularly prevalent in SMA patients or mice models (save for congenital structural defects),⁴¹ SMA I patients with artificially prolonged lifespans have been shown to exhibit autonomic dysfunction,⁴² which may benefit from peripheral restoration of SMN.

Peripheral rescue of SMA may not be properly resolved by CNS administration alone, and tcDNA's uptake profile across all tissues is a potential solution to this issue. That being said, other promising candidates which offer a similar uptake profile using systemic administration including vector- and AON-based strategies are currently under investigation.

Many AAV vectors have been shown to efficiently cross the BBB,⁴³ and as an example a group using self-complementary- adeno-associated vector serotype 9 (scAAV9) has demonstrated transduction efficacy throughout the spinal cord after a single systemic injection in newborn and adult mice and non-human primates, potentially surmounting the issue of peripheral vs. central treatment of SMA.^{44,45} A clinical trial aiming at replacing SMN1 directly, using these vectors is currently underway (ClinicalTrials.gov Identifier: NCT02122952).

However, the well-documented immunogenicity of the AAV capsid is likely to complicate repeated administration (if required) of such a therapy, not an issue with AON-based approaches. Combined treatments consisting of an initial AAV injection followed by sequential AON administration could be a viable treatment approach.

Recently a peptide-conjugated PMO AON (Pip6a-PMO) has been administered intravenously in SMA mice at P0 and P2, achieving significant lifespan extension.⁴⁶ More importantly, this group demonstrated corrected SMN2 transcripts in the CNS after tail vein administration at 7.5 weeks, suggesting that this AON may penetrate the BBB. However, this was demonstrated in an asymptomatic mouse model, thus TCI7 is the only AON to demonstrate geno- and pheno-typic correction of central and peripheral SMA pathology with systemic administration as late as P7. Furthermore, the peptide moiety of Pip6a-PMO may be more likely to induce immunological reactions upon systemic administration vs. the naked chemistry of tcDNA, rendering clinical translation a lengthier and more complex process.

It is still debated how SMN deficiency leads to peripheral pathology, but the major goal of a tcDNA-based therapeutic strategy is to achieve systemic efficacy to ensure the best resolution of disease in SMA patients. TcDNA's proven efficacy in restoring SMN2 exon 7 reinclusion in addition to its unique uptake profile and naked chemistry, offers these properties following less invasive administration, without the need for patient anaesthesia. TcDNA could therefore represent a particularly attractive AON therapy for SMA requiring whole-body treatment.

MATERIAL AND METHODS

Cell culture and tcDNA transfection

Human fibroblasts from a 3-year old type I SMA patient (GM03813, Coriell Cell Repositories) and wild type fibroblasts (GM03814, Coriell Cell Repositories) were grown in Dulbecco's modified Eagle Medium with 20% foetal bovine serum and 1% penicillin-streptomycin (100 U/ml). TcDNA AONs were synthesised by Synthena as previously described^{47,48} and 2'OMePS were obtained from Eurogentec. The two sequences used are SMN2 TSL (39;55) 5'-(pTTAATTTAAGGAATGTG)-3' and SMN2 TCI7(10;24) 5'-(pCTTTCATAATGCTGG)-3'.

2'OMePS and tcDNA transfection were performed with oligofectamine (Invitrogen) and incubated for 48 hours without serum and antibiotics.

RT-PCR and qRT-PCR

Total RNA was extracted 48 hours post-transfection using TRIzol reagent (Invitrogen) and first-strand cDNA synthesis was performed using Super Script II (Invitrogen) and random hexamers. PCR reactions were carried out with Master Mix 2x Phusion GC (Finnzymes) in a total volume of 50 μ L from 200ng cDNA, with 10 μ M each of the SMN-Ex6-FW (5'-GCTGATGCTTTGGGAAGTATGTTA-3') and SMN-Ex8-Re primers (5'-ATTCCAGATCTGTCTGATCG-3'). The PCR products were separated by electrophoresis on a 3% agarose gel.

Real-time quantitative PCR reactions were run in Opticon2 (Biorad). cDNA was used as a template with primers specific for SMN and GAPDH, a housekeeping gene used as control for variations in the amount of template loaded to each reaction. The SMN primers, forward 5'-GCTGATGCTTTGGGAAGTATGTTA-3' in exon 6 and reverse 5'-CCTTAATTTAAGGAATGTGAGCACC-3' in exon 7 were used. 20 ng of cDNA were included in a 20 μ L-mix containing iTaq Universal SYBR[®] green supermix (Biorad) and 0,2 μ M of each specific primer. The run conditions were as follow: 15 min 95°C polymerase activation step, followed by 50 cycles of 2-step qPCR (15 sec of 95°C denaturation, 1 min of 60°C combined annealing/extension)

Western blot

Fibroblast protein extracts were obtained in lysis buffer (10 mmol/l HEPES pH 7.9, 100 mmol/l KCl, 1 mmol/l EDTA, 1 mmol/l 1,4-dithiothreitol, 1 \times complete protease inhibitor cocktail (Roche), 0.5% NP-40). Equal amounts of protein (determined by Bradford Protein Assay (Pierce)) were mixed with 2 \times loading buffer (125 mmol/l Tris pH 6.8, 2% sodium dodecyl sulfate, 10% glycerol, 0.01% bromophenol blue, 10% β -mercaptoethanol).²⁵ 10 μ g of protein of each sample were resolved by SDS-PAGE 4-12% Bis-Tris Gels (Invitrogen) and transferred onto a nitrocellulose membrane. The membrane was blocked with 10% milk in

Phosphate-Buffered Saline-Tween buffer. SMN immunoblot was performed overnight using rabbit polyclonal antibody SMN H-195 (dilution 1/500, Santa Cruz). A goat anti-rabbit secondary antibody conjugated with horseradish peroxidase was used to detect the protein SMN (dilution 1/50,000). Signals were detected with the SuperSignal West Pico Chemiluminescent kit (ThermoScientific). The membrane was then washed, re-blocked and probed with mouse monoclonal anti-actin (dilution 1/5000, Sigma Aldrich) followed by a secondary sheep anti-mouse conjugated with horseradish peroxidase (dilution 1/15,000). The signal was detected as described earlier. Membranes were converted to numerical pictures by scanning and band intensities were analyzed using the ImageJ 1.46r software (<http://rsb.info.nih.gov/gate2.inist.fr/ij/>) and normalised to actin protein.

Immunofluorescence

Transfected fibroblasts on slides were fixed with acetone/methanol (volume/volume). Fixed cells were blocked in PBS + 5% BSA for 1 hour. SMN immuno-staining was performed with rabbit polyclonal antibody SMN h-195 (dilution 1/100 in PBS +1% BSA) for 1 hour. Cells were washed in PBS and incubated with a secondary anti-rabbit Alexa 594. Then, cells were washed in PBS and incubated 5 minutes with DAPI (dilution 1/50,000). Slides were then fitted with cover slips using Fluoromount-G (SouthernBiotech), and incubated overnight at 4°C.

Animal experiments

All procedures were performed in accordance with national and European legislation. All mice experiments were carried out at the Centre d'évaluation fonctionnelle, Université Pierre

et Marie Curie, Paris, France. The initial breeding SMA type III model mice were purchased from Jackson Laboratory after MTA accordance, and were originally developed by Hsieh-Li et al.²⁴ We used strain FVB.Cg- Tg(SMN2)2HungSMN1tm1Hung/J, founder line 2, stock number 005058. TC17 oligonucleotides were administered weekly to SMA mice by subcutaneous (Sc) injections at a dose of 200mg/kg/wk under general anaesthesia using isoflurane, starting at 7 days of age. Treated mice were sacrificed at various time points as indicated in the results section and muscles and tissues were harvested and snap-frozen in liquid nitrogen-cooled isopentane and stored at -80°C before further analysis.

Respiratory function

Mouse respiratory function was evaluated by whole-body plethysmography using an 'EMKA Technologies' plethysmograph as described by TREAT-NMD (http://www.treat-nmd.eu/downloads/file/sops/dmd/MDX/DMD_M.2.2.002.pdf). Briefly, unrestrained conscious mice were placed in calibrated chambers containing a pneumatograph that measured pressure differentials within the compartment by a difference in air flow. Mice were allowed to acclimate in chambers for 45 min at a stable temperature and humidity. Data were then collected every 5s using 'iox' software (EMKA technologies). The inspiration time T_i was defined as the start of inspiration to the end of inspiration and the expiration time was defined as the start of expiration to the end of expiration. The relaxation time RT was defined as the time from the start of expiration to the time when 65% of the total expiratory pressure occurred. $Pause$ and $Penh$ were defined and calculated by the following formulas: $Pause = (T_e - RT)/RT$ and $Penh = (PEP/PIP) \times Pause$, where PEP is peak expiratory pressure and PIP is peak inspiratory pressure. The value of each parameter was calculated from an average of 60 recordings of 5 sec representing a total of 5 min. Inclusion criteria for each recording were > 8 respiration events by 5 sec and $>80\%$ of success rate as measured by the iox software.

Statistical analysis

Data were analysed by GraphPad Prism5 software (San Diego, California, USA) and shown as the means \pm S.E.M. “*n*” refers to the number of mice per group. Comparisons of statistical significance were assessed by unpaired student t-tests. Significant levels were set at *P < 0.05, **P < 0.01, ***P < 0.001.

1. Lefebvre, S. et al. Identification and characterization of a spinal muscular atrophy-determining gene. *Cell* 80, 155-65 (1995).
2. Liu, Q. & Dreyfuss, G. A novel nuclear structure containing the survival of motor neurons protein. *Embo J* 15, 3555-65 (1996).
3. Pellizzoni, L., Yong, J. & Dreyfuss, G. Essential role for the SMN complex in the specificity of snRNP assembly. *Science* 298, 1775-9 (2002).
4. Fallini, C., Bassell, G. J. & Rossoll, W. Spinal muscular atrophy: the role of SMN in axonal mRNA regulation. *Brain Res* 1462, 81-92 (2012).
5. Feldkotter, M., Schwarzer, V., Wirth, R., Wienker, T. F. & Wirth, B. Quantitative analyses of SMN1 and SMN2 based on real-time lightCycler PCR: fast and highly reliable carrier testing and prediction of severity of spinal muscular atrophy. *Am J Hum Genet* 70, 358-68 (2002).
6. Lorson, C. L., Hahnen, E., Androphy, E. J. & Wirth, B. A single nucleotide in the SMN gene regulates splicing and is responsible for spinal muscular atrophy. *Proc Natl Acad Sci U S A* 96, 6307-11 (1999).
7. Monani, U. R. et al. A single nucleotide difference that alters splicing patterns distinguishes the SMA gene SMN1 from the copy gene SMN2. *Hum Mol Genet* 8, 1177-83 (1999).
8. Lorson, C. L. et al. SMN oligomerization defect correlates with spinal muscular atrophy severity. *Nat Genet* 19, 63-6 (1998).
9. Pellizzoni, L., Charroux, B. & Dreyfuss, G. SMN mutants of spinal muscular atrophy patients are defective in binding to snRNP proteins. *Proc Natl Acad Sci U S A* 96, 11167-72 (1999).
10. Butchbach, M. E. Copy Number Variations in the Survival Motor Neuron Genes: Implications for Spinal Muscular Atrophy and Other Neurodegenerative Diseases. *Front Mol Biosci* 3, 7 (2016).
11. Scholl, R., Marquis, J., Meyer, K. & Schumperli, D. Spinal muscular atrophy: position and functional importance of the branch site preceding SMN exon 7. *RNA Biol* 4, 34-7 (2007).
12. Singh, N. N., Androphy, E. J. & Singh, R. N. In vivo selection reveals combinatorial controls that define a critical exon in the spinal muscular atrophy genes. *Rna* 10, 1291-305 (2004).
13. Singh, N. N., Androphy, E. J. & Singh, R. N. An extended inhibitory context causes skipping of exon 7 of SMN2 in spinal muscular atrophy. *Biochem Biophys Res Commun* 315, 381-8 (2004).
14. Singh, N. K., Singh, N. N., Androphy, E. J. & Singh, R. N. Splicing of a critical exon of human Survival Motor Neuron is regulated by a unique silencer element located in the last intron. *Mol Cell Biol* 26, 1333-46 (2006).

15. Singh, N. N., Singh, R. N. & Androphy, E. J. Modulating role of RNA structure in alternative splicing of a critical exon in the spinal muscular atrophy genes. *Nucleic Acids Res* 35, 371-89 (2007).
16. Hua, Y., Vickers, T. A., Okunola, H. L., Bennett, C. F. & Krainer, A. R. Antisense masking of an hnRNP A1/A2 intronic splicing silencer corrects SMN2 splicing in transgenic mice. *Am J Hum Genet* 82, 834-48 (2008).
17. Hua, Y. et al. Antisense correction of SMN2 splicing in the CNS rescues necrosis in a type III SMA mouse model. *Genes Dev* 24, 1634-44 (2010).
18. Hua, Y. et al. Peripheral SMN restoration is essential for long-term rescue of a severe spinal muscular atrophy mouse model. *Nature* 478, 123-6 (2011).
19. Porensky, P. N. et al. A single administration of morpholino antisense oligomer rescues spinal muscular atrophy in mouse. *Hum Mol Genet* 21, 1625-38 (2012).
20. Zhou, H. et al. A novel morpholino oligomer targeting ISS-N1 improves rescue of severe spinal muscular atrophy transgenic mice. *Hum Gene Ther* 24, 331-42 (2013).
21. Osman, E. Y. et al. Morpholino antisense oligonucleotides targeting intronic repressor Element1 improve phenotype in SMA mouse models. *Hum Mol Genet* 23, 4832-45 (2014).
22. Renneberg, D., Bouliong, E., Reber, U., Schumperli, D. & Leumann, C. J. Antisense properties of tricyclo-DNA. *Nucleic Acids Res* 30, 2751-7 (2002).
23. Goyenvalle, A. et al. Functional correction in mouse models of muscular dystrophy using exon-skipping tricyclo-DNA oligomers. *Nat Med* 21, 270-5 (2015).
24. Hsieh-Li, H. M. et al. A mouse model for spinal muscular atrophy. *Nat Genet* 24, 66-70 (2000).
25. Marquis, J. et al. Spinal muscular atrophy: SMN2 pre-mRNA splicing corrected by a U7 snRNA derivative carrying a splicing enhancer sequence. *Mol Ther* 15, 1479-86 (2007).
26. LoMauro, A. et al. Alterations of thoraco-abdominal volumes and asynchronies in patients with spinal muscle atrophy type III. *Respir Physiol Neurobiol* 197, 1-8 (2014).
27. Chiriboga, C. A. et al. Results from a phase 1 study of nusinersen (ISIS-SMN(Rx)) in children with spinal muscular atrophy. *Neurology* 86, 890-7 (2016).
28. Hache, M. et al. Intrathecal Injections in Children With Spinal Muscular Atrophy: Nusinersen Clinical Trial Experience. *J Child Neurol* 31, 899-906 (2016).

29. Passini, M. A. et al. CNS-targeted gene therapy improves survival and motor function in a mouse model of spinal muscular atrophy. *J Clin Invest* 120, 1253-64 (2010).
30. Meyer, K. et al. Rescue of a severe mouse model for spinal muscular atrophy by U7 snRNA-mediated splicing modulation. *Hum Mol Genet* 18, 546-55 (2009).
31. Araujo, A., Araujo, M. & Swoboda, K. J. Vascular perfusion abnormalities in infants with spinal muscular atrophy. *J Pediatr* 155, 292-4 (2009).
32. Rudnik-Schoneborn, S. et al. Digital necroses and vascular thrombosis in severe spinal muscular atrophy. *Muscle Nerve* 42, 144-7 (2010).
33. Somers, E., Stencel, Z., Wishart, T. M., Gillingwater, T. H. & Parson, S. H. Density, calibre and ramification of muscle capillaries are altered in a mouse model of severe spinal muscular atrophy. *Neuromuscul Disord* 22, 435-42 (2012).
34. Borisov, A. B., Huang, S. K. & Carlson, B. M. Remodeling of the vascular bed and progressive loss of capillaries in denervated skeletal muscle. *Anat Rec* 258, 292-304 (2000).
35. Hua, Y. et al. Motor neuron cell-nonautonomous rescue of spinal muscular atrophy phenotypes in mild and severe transgenic mouse models. *Genes Dev* 29, 288-97 (2015).
36. Martinez, T. L. et al. Survival motor neuron protein in motor neurons determines synaptic integrity in spinal muscular atrophy. *J Neurosci* 32, 8703-15 (2012).
37. Sahashi, K. et al. Pathological impact of SMN2 mis-splicing in adult SMA mice. *EMBO Mol Med* 5, 1586-601 (2013).
38. Henrichsen, T. et al. Perfluorodecalin lavage of a longstanding lung atelectasis in a child with spinal muscle atrophy. *Pediatr Pulmonol* 47, 415-9 (2012).
39. Leistikow, E. A. et al. Migrating atelectasis in Werdnig-Hoffmann disease: pulmonary manifestations in two cases of spinal muscular atrophy type 1. *Pediatr Pulmonol* 28, 149-53 (1999).
40. Schreml, J. et al. Severe SMA mice show organ impairment that cannot be rescued by therapy with the HDACi JNJ-26481585. *Eur J Hum Genet* 21, 643-52 (2012).
41. Rudnik-Schoneborn, S. et al. Congenital heart disease is a feature of severe infantile spinal muscular atrophy. *J Med Genet* 45, 635-8 (2008).
42. Hachiya, Y. et al. Autonomic dysfunction in cases of spinal muscular atrophy type 1 with long survival. *Brain Dev* 27, 574-8 (2005).

43. Hocquemiller, M., Giersch, L., Audrain, M., Parker, S. & Cartier, N. Adeno-Associated Virus-Based Gene Therapy for CNS Diseases. *Hum Gene Ther* 27, 478-96 (2016).
44. Duque, S. et al. Intravenous administration of self-complementary AAV9 enables transgene delivery to adult motor neurons. *Mol Ther* 17, 1187-96 (2009).
45. Foust, K. D. et al. Rescue of the spinal muscular atrophy phenotype in a mouse model by early postnatal delivery of SMN. *Nat Biotechnol* 28, 271-4 (2010).
46. Hammond, S. M. et al. Systemic peptide-mediated oligonucleotide therapy improves long-term survival in spinal muscular atrophy. *Proc Natl Acad Sci U S A* 113, 10962-7 (2016).
47. Wagner, T. & Pfeleiderer, W. Synthesis of 2'-deoxyribonucleoside 5'-phosphoramidites: New building blocks for the inverse (5'-3')-oligonucleotide approach. *Helvetica Chimica Acta* 83, 2023-2035 (2000).
48. Renneberg, D. & Leumann, C. J. Watson-Crick base-pairing properties of tricyclo-DNA. *J Am Chem Soc* 124, 5993-6002 (2002).

AUTHOR CONTRIBUTIONS

V.R, G.G., and A.G. designed and performed the laboratory experiments. V.R. analysed the experiments. V.R., J.P., C.L., L.G., and A.G. wrote the manuscript. V.R. and A.G. conceived the project, designed the experiments, supervised the entire study, and will serve as corresponding authors.

ACKNOWLEDGEMENTS

This work was supported by the Agence Nationale de la Recherche (Chair of Excellence HandiMedEx), the Association Monegasque contre les Myopathies, the Duchenne Parent Project France, and by the Institut National de la Santé et de la Recherche Médicale (INSERM).

COMPETING FINANCIAL INTERESTS

Christian Leumann and Luis Garcia are co-funders of Synthena, which produces tricyclo-DNA oligomers

Figure 1: Evaluation of *in vitro* efficiency of tricyclo-DNA TCI7

a) Detection of the inclusion of exon 7 of SMN2 mRNA by RT-PCR (primers on exons 6 and 8) in patient SMA I fibroblasts. PCR products are visualized on 3% agarose gel (top) and quantified by imageJ (bottom). TCI7: fibroblasts treated with tcDNA AONs targeting the ISS-N1, (SMAI) Untreated SMAI fibroblasts (GM03813 Coriell), (WT) healthy fibroblasts of mother (GM03814 Coriell). **b)** Detection of the SMN protein by Western blot in fibroblasts and normalisation with actin. Lane 1: Untreated SMAI fibroblasts (GM03813 Coriell), Lane 2: SMA fibroblasts treated with TCI7, Lane 3: healthy fibroblasts of mother (GM03814 Coriell) Errors bars represent standard deviations. (*) $p < 0.05$; (**) $p < 0.01$. **c)** Detection of the SMN protein by immunostaining in untreated SMA fibroblasts (top) and SMA fibroblasts transfected with TCI7 (bottom). Cells were immunostained with the polyclonal antibody H-SMN 195 (Santacruz). The red staining shows the expression of SMN protein in gems. Nuclei are labeled in blue (Dapi). Left panel: magnification x20; right panel: magnification x63. For magnification (x63), the apotome is used to see the gems in the nucleus. **d)** Counting of the gem number positive for SMN per nucleus (n=100 nuclei). The black bars correspond to untreated SMA type I, and grey to treated cells with TCI7.

Figure 2: Evaluation of tricyclo-DNA TCI7 efficiency in SMA mice.

Detection of the inclusion of exon 7 of SMN2 mRNA by RT-PCR in different tissues (a. Gastrocnemius, b. Diaphragm, c. Heart, d. Brain, e. Spinal cord) of SMA mice type III and quantification using Image J (bottom). (Un) untreated mice (n=3), (4wk) mice treated during 4 weeks with 200 mg/kg/wk by subcutaneous injection and sacrificed 2 weeks after treatment (n=3), (12wk) mice treated during 12 weeks with 200 mg/kg/wk by subcutaneous injection and sacrificed 2 weeks after treatment (n=4).

Errors bars represent standard deviations. (*) $p < 0.05$; (**) $p < 0.01$, compared with saline controls.

Figure 3: Quantitative evaluation of exon 7 inclusion after tricyclo-DNA TCI7 treatment in SMA mice.

Detection of the inclusion of exon 7 of SMN2 mRNA by qPCR in heart and brain of SMA type III mice. The primers used for amplification are located on exon 6 and 7 and normalized with GAPDH. (Un) untreated mice, (4wk) mice treated during 4 weeks with 200 mg/kg/wk by subcutaneous injection of TCI7, (12wk) mice treated during 12 weeks with 200 mg/kg/wk by subcutaneous injection of TCI7; $n = 3$ per group.

Figure 4: Sustained effect of tricyclo-DNA TCI7 treatment in SMA mice.

Detection of the inclusion of exon 7 of SMN2 mRNA by RT-PCR in different tissues (Gastrocnemius, Diaphragm, Heart, Brain, Spinal cord) of SMA mice type III and quantification using Image J to evaluate the long term effect of tcDNA treatment.

Black bars: untreated mice, grey bars mice treated during 4 weeks with 200 mg/kg/wk by subcutaneous injection and sacrificed 2 weeks after treatment (called 4wk/2wk), dark grey bars mice treated during 4 weeks with 200 mg/kg/wk by subcutaneous injection and sacrificed 10 weeks after treatment (called 4wk/10wk). $n = 3$ per group; errors bars represent standard deviations. (*) $p < 0.05$; (**) $p < 0.01$.

Figure 5: Respiratory function evaluation in SMA mice after tricyclo-DNA TCI7 treatment.

Respiratory function in *SMA* mice treated with 200 mg/kg of tcDNA for 12 weeks, compared to *SMA* control mice and WT mice ($n = 4$ per group). T_i , T_e , EIP, EEP, RT, f , penh are shown. Error bars are mean \pm standard deviation. (*) $p < 0.05$ compared with the saline controls.

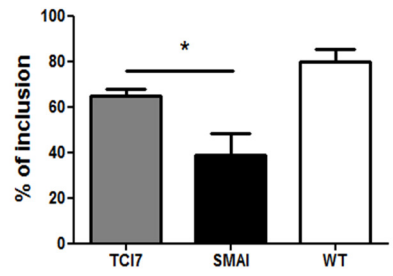
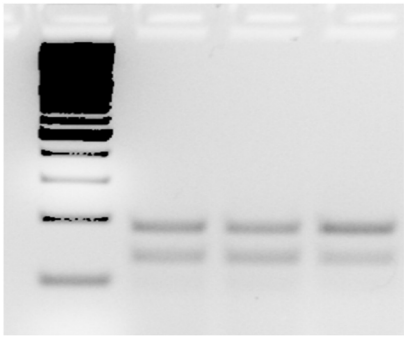
Figure 6: **Phenotype rescue following tricyclo-DNA treatment in SMA mice.**

a) Phenotypic rescue in type III *SMA* mice at 12 weeks of age after tcDNA treatment, compare to *SMA* control. **b)** Toes and tails necrosis rescue in treated mice (right picture) compared to *SMA* control (left picture). **c)** Ears rescue in treated mice (right picture) compare to *SMA* control (left picture) **d)** Tails length of mice according to weeks. The darker grey curve corresponds to the size of the tails of type III *SMA* mice treated with TcI7 during 12 weeks ($n=4$), the black curve is the size of the tails of type III *SMA* untreated mice ($n=11$) and the lighter grey one corresponds to the tails length of type III *SMA* mice treated with TcI7 during 4 weeks only ($n=3$).

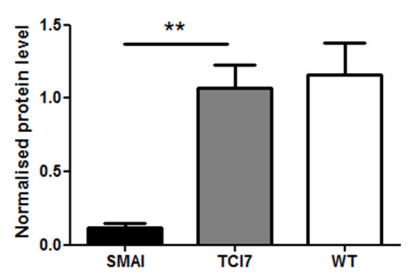
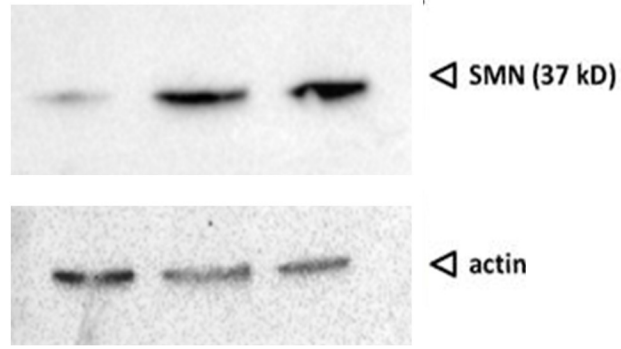
Table 1: **Respiratory function evaluation in wild-type mice FVB and SMA mice type III.**

		T_i (msec)	T_e (msec)	PIF (ml/s)	PEF (ml/s)	TV (ml)	EV (ml)	RT (msec)	MV (ml)	f (bpm)	EIP (msec)	EEP (msec)	Penh
FVB	mean	129,6	180,8	2,9	1,9	0,2	0,2	109,5	44,4	205,5	1,2	19,9	0,444
	sem	7,18	50,45	0,30	0,33	0,03	0,03	37,71	8,68	20,47	0,17	4,37	0,061
SMA	mean	130,1	242,8	2,4	1,3	0,2	0,2	157,5	33,3	179,0	1,2	23,4	0,353
	sem	8,81	29,20	0,35	0,23	0,01	0,01	22,48	5,23	15,41	0,08	2,40	0,026
p value		0,5130	0,0472	0,4490	0,0747	0,1816	0,2039	0,0423	0,1400	0,1136	0,8545	0,1899	0,0097
		=	+	=	=	=	=	+	-	-	=	+	-

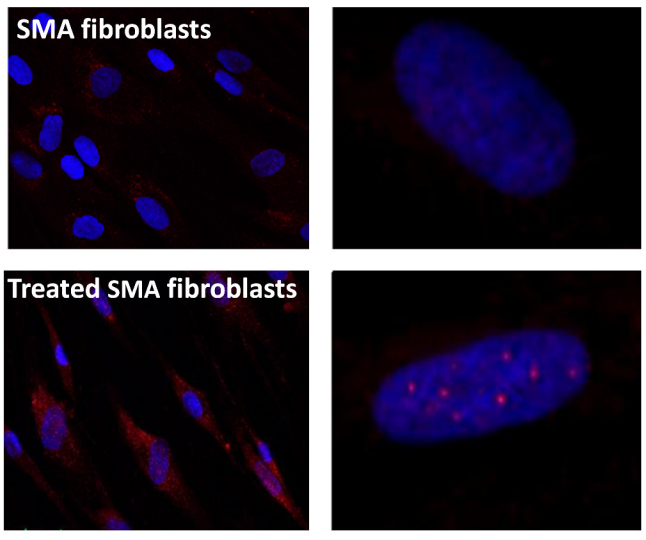
a TCI7 SMAI WT



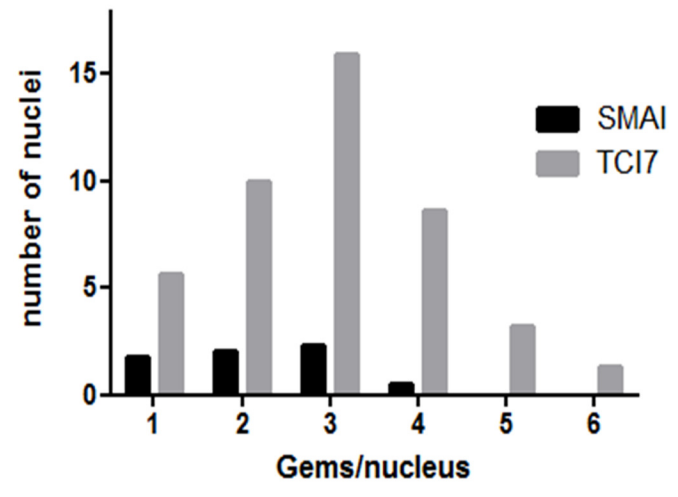
b SMAI TCI7 WT



c



d



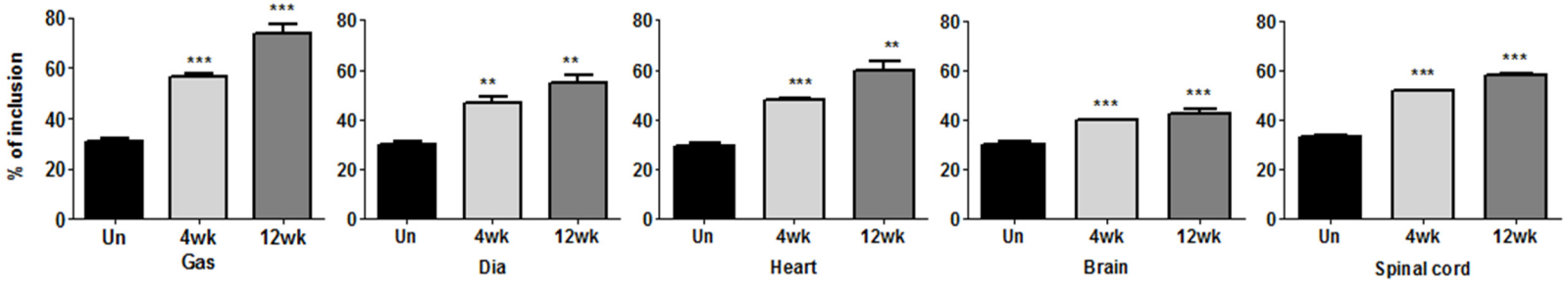
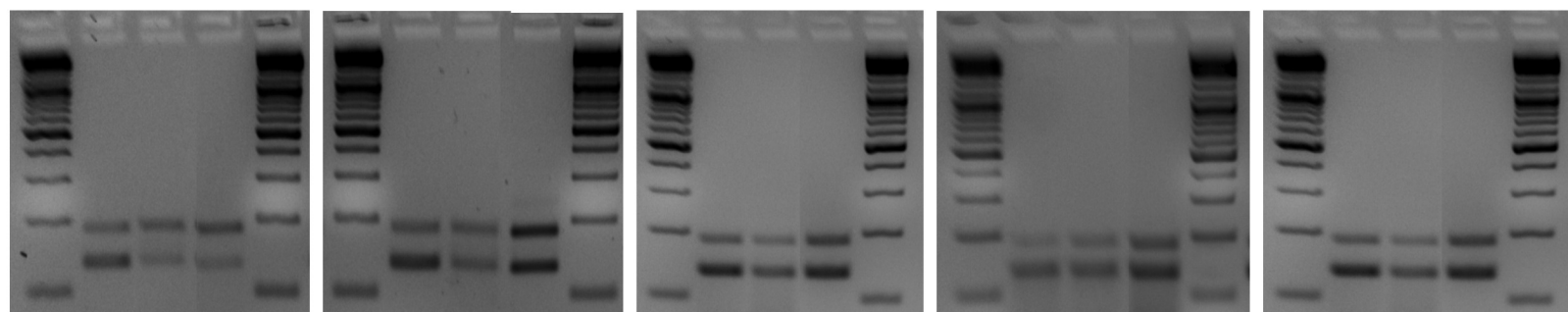
a GAS
Un 4wk 12wk

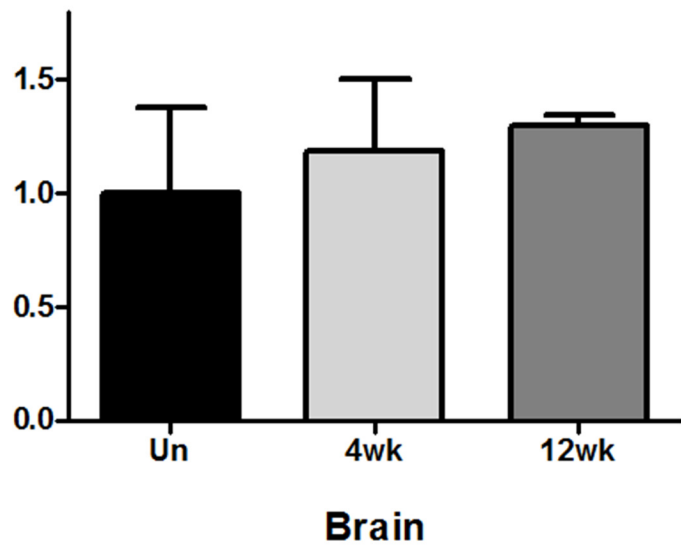
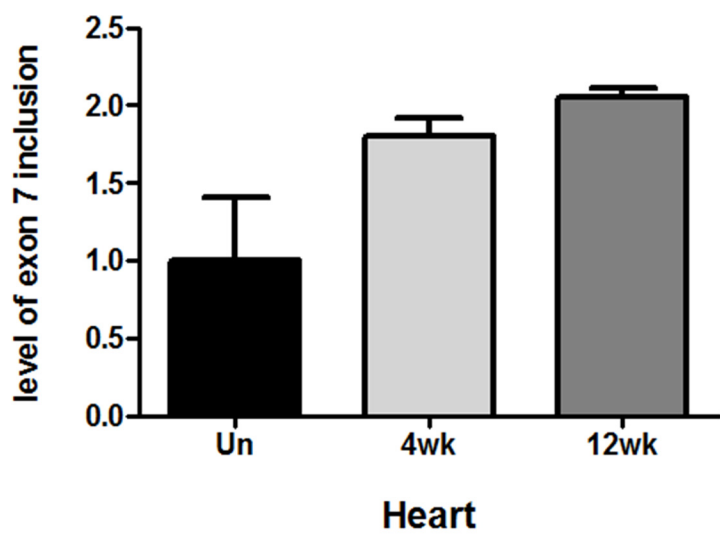
b Dia
Un 4wk 12wk

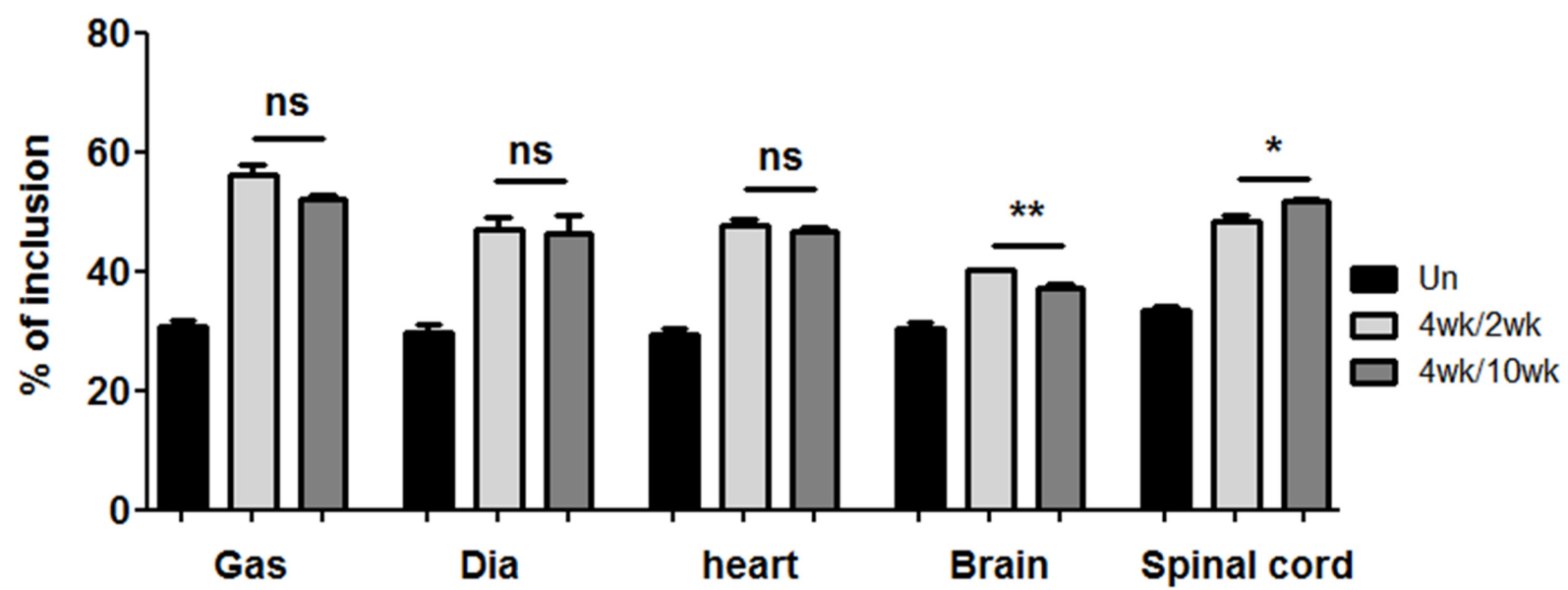
c Heart
Un 4wk 12wk

d Brain
Un 4wk 12wk

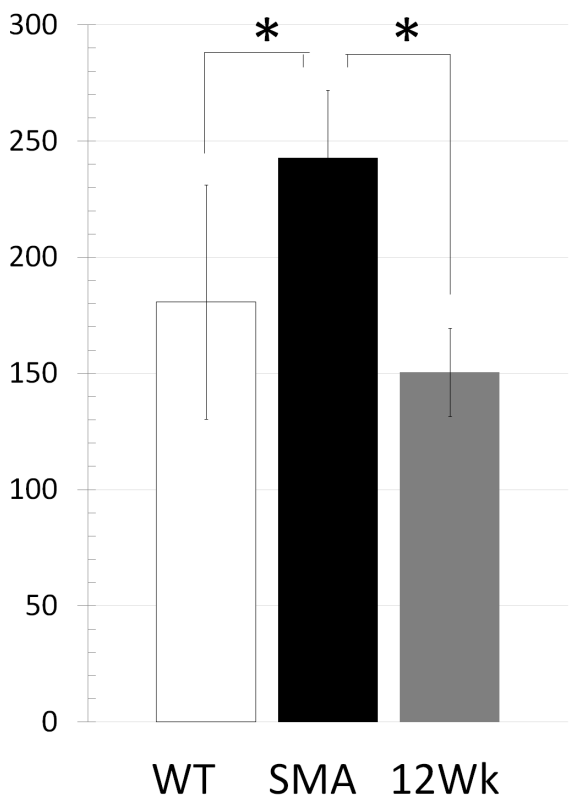
e Spinal cord
Un 4wk 12wk



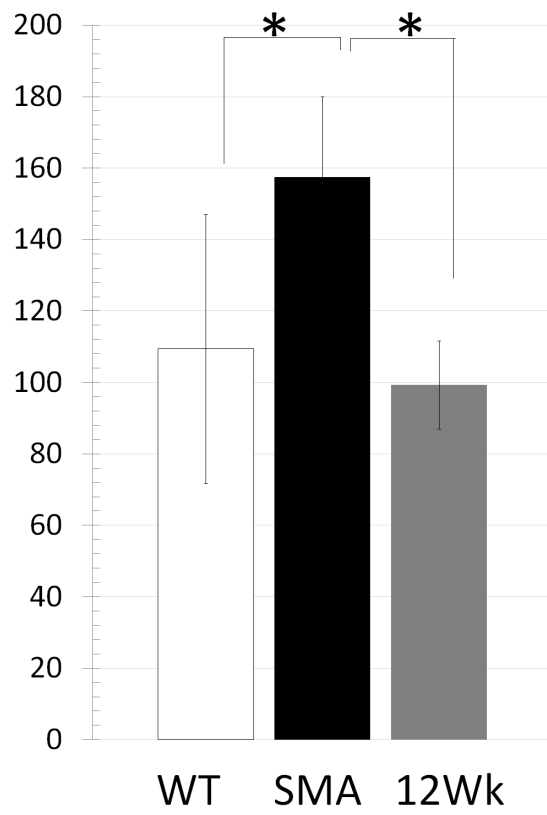




Te (msec)



RT (msec)



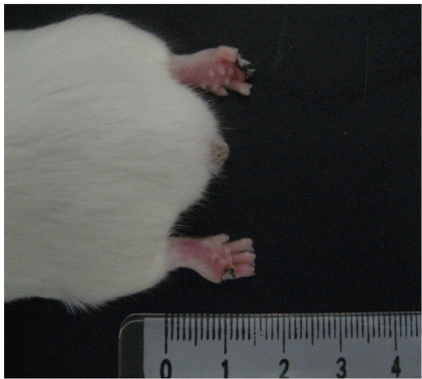
Untreated mice

tcDNA treated mice

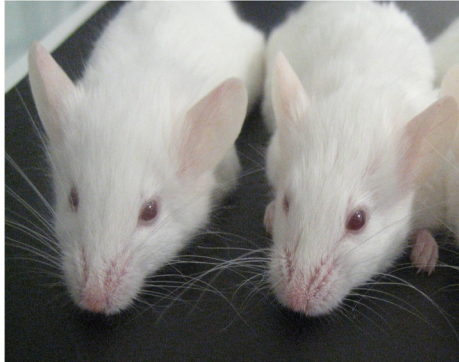
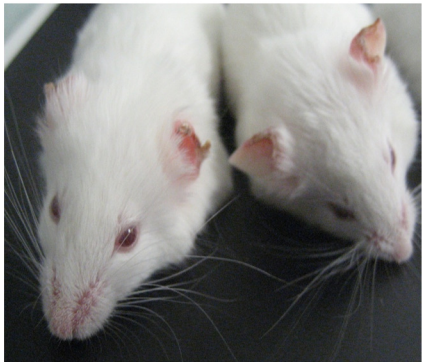
a



b



c



d

